ANALYTICAL APPROXIMATION OF ATMOSPHERIC CORRECTION IN RUGGED TERRAIN

Harriet H. Kagiwada
Applied Research Center for Systems Science
School of Engineering and Computer Science
California State University, Fullerton, U.S.A.
S. Ueno
Information Science Laboratory
Kyoto School of Computer Science
Tanakamonzencho 7, Sakyoku Kyoto 606, Japan
Y. Kawata
Information Science Laboratory
Kanazawa Institute of Technology
Nonoichimachi, Ishikawa 921, Japan

ABSTRACT

The apparent radiance of surface features which an arbitrary spacecraft measures differs from the intrinsic surface radiance of the object, because of the presence of intervening terrestrial atmosphere bounded below by the horizontally nonuniform albedos of non-Lambertian surface in rugged terrain. The removal of such atmospheric effects on remotely sensed data improves the accuracy of the classification of the ground objects not only in the unitemporal but also in the multitemporal images. The applications for these data have been found in many disciplines, but their usefulness in areas of mountainous terrain is limited by the topographic effect on deblurring, i.e., the effect of terrain orientation on the determination of the ground reflectance law.

In the present paper it is shown how to solve approximately and effectively the boundary conditions in rugged terrain. It is physically approximated using a global approach that includes (i) the effect of terrain orientation, consisting of the direct and diffuse radiation in connection with shadow, (ii) the irradiance effect from the adjacent terrain, and other effect. Such physical reduction seems to be tractable so that the simultaneous solution of the nonlinear Riccati-type integro-differential equations governing the scattering and transmission functions with the topography-dependent boundary conditions is numerically carried out via the high-speed digital computers.

Key Words: Atmospheric correction, topographic effect, rugged terrain.

INTRODUCTION

In the theory of radiative transfer, the angular distribution of radiation emergent from the top of the finite, vertically inhomogeneous and anisotropically scattering atmosphere bounded below by the horizontally inhomogeneous albedos of the ground has been theoretically and approximately discussed by several authors (cf. [2], [3], [5] ~ [14], [16] ~ [19], [21], [22], [24] ~ [30]). Up to now the approximate solutions of the multidimensional transfer equation have been analytically and numerically implemented. However, the topographic effect on the spectral intensity of radiation from space has not been so analytically evaluated, because of the difficulty of solving simultaneously the equation of radiative transfer, together with the boundary condition based on an interaction of radiation due to effect of the terrain orientation and the adjacent slopes. In this paper it will be theoretically shown how to compute effectively the topographic effect on the satellite-level luminance observations, i.e., the effect of solar position, atmospheric composition, terrain orientation and adjacent slopes on spectral response from nadir-pointing sensors.

BASIC EQUATIONS

In the case of rugged terrain, the effect of atmospheric attenuation is extremely variable. Under good visibility conditions we can build an atmospheric model, governing the amount and distribution of the scattered light. However, an interaction of atmospheric radiation with the ground gives rise to difficulties due to the reflectance properties of the ground and its topographic shape. Because of the difficulty of an independent analysis of the light attenuation in the atmosphere and on the ground, only under certain circumstances could both processes be analyzed separately.

While the ground in flat terrain can be thought to be horizontal, in mountainous terrain the combined effect of reflection processes and surface orientation should be allowed for. In other words, in addition to the atmospheric attenuation effect, we should allow for the variable surface orientations and its structures, which are the properties of mountainous terrain covered with vegetation (or soils). It should be mentioned that an allowance for the topographic effect is limited because of the computational difficulty of determining exactly all the reflection properties in rugged terrain.

In this section we consider a three-dimensional radiative transfer model consisting of an atmosphere bounded below by a non-flat reflecting layer with nonuniform albedo distribution. Suppose that the top $z=z_1$ of a plane-parallel, vertically inhomogeneous, anisotropically scattering atmosphere of an optical thickness τ_1 is uniformly and monodirectionally illuminated by parallel rays of a constant net flux πF per unit area normal to the direction of propagation. Let the upwelling intensity of radiation emergent in the direction Ω from the level $z(0 \le z \le z_1)$ at horizontal rectangular coordinates $(-\infty < x, y < \infty)$ be denoted by $I(z,x,y,+\Omega)$. In the above Ω stands for $(\Theta = \cos^{-1} v, \phi)$, where Θ is a polar angle measured from the outward normal and ϕ is an azimuthal angle with respect to an arbitrary horizontal axes. Let the level-dependant phase function be denoted by $p(z;\Omega,\Omega')$. The equation of transfer appropriate to this case, i.e., governing the diffuse radiation field takes the form

$$\Omega \cdot \nabla I(z,x,y;\Omega) + \alpha(z) I = J(z,x,y;\Omega) \qquad (1)$$

where $\infty < x, y < \infty$, $d\Omega' = dv' d\phi'$, and $\Omega \cdot \nabla I$ is the directional derivative of I in the direction Ω, and the J-function is the source function, depending on the coordinate and the face direction.

The source function takes the form given below

$$J(z,x,y;\Omega) = \frac{\sigma(z)}{4\pi} \int_{-1}^{+1} \int_{0}^{2\pi} p(z,\Omega,\Omega') I(z,x,y;\Omega') d\Omega' + \frac{\sigma(z)}{4} F e^{-\tau/u} p(z,\Omega,\Omega_0) + \frac{\sigma(z)}{4\pi} \int_{0}^{1} \int_{0}^{2\pi} e^{-(\tau s - \tau)/w} p(z,\Omega,\Omega') R (z_s, x_s, y_s, \Omega') d\Omega' \qquad (2)$$

In Eq. (2) $\sigma(z)$ = the volume level-dependent scattering coefficient and the phase angle 4π under the integral sign represents an integration of the integrands with respect to the polar angle from 0 to π and that with respect to the azimuth over the whole horizontal angle.

Furthermore, τ(or τ_s) is the optical depth corresponding to the altitude z(or z_s); the optical thickness τ_1 is often used as an independent variable instead of the geometrical thickness z_1. In Eq. (2) the $R(z_s,x_s,y_s;\Omega)$-function is the radiation quantity emitted in the direction $\Omega(\Theta,\phi)$ from the target point (z_s,x_s,y_s) on the rugged terrain. The R-function takes the form

$$R(z_s,x_s,y_s;\Omega)=\frac{1}{\pi}\int_0^1\int_0^{2\pi} \rho(z_s,x_s,y_s;\Omega,\Omega') \times$$
$$\times\ I(z_s,x_s,y_s;-\Omega')v'dv'd\phi'+uFe^{-\tau s/u}$$
$$\rho(z_s,x_s,y_s;\Omega_0,\Omega), \quad (3)$$

where ρ is the bidirectional reflectance function and furthermore I-function is the downwards intensity of radiation at the target (x_s,y_s,z_s).

In order to accurately classify the sensed radiance data, i.e., the satellite-level radiance of a high spatial resolution, we should allow for such factors as target position (z_s,x_s,y_s), polar and azimuthal angles (Θ_s,ϕ_s) and the bidirectional spectral reflectance of these surfaces, in addition to the solar position, atmospheric composition, and the adjacency effect (i.e., the reflectance of the surrounding).

Such global information is contained in the form of isoelevation contour lines in geological maps and also in the digital terrain data on a computer compatible magnetic tapes. In the case of high-altitude imagery the radiometric correction due to the peculiarity of the reflectance characteristics seems to be small compared with that due to the low altitude imagery.

In Eq.(3) the bidirectional reflectance law at the target changes horizontally and vertically. In other words it is assumed that the reflection at each point x_s,y_s on the ground z_s is expressed in terms of the bidirectional reflectance function (BDRF) ρ. The ρ-function defines the angular reflectance law at each point on the ground, i.e., the probability distribution of reflection from an incident direction $-\Omega'$ into direction Ω. In other words, the scattered photons in the flat terrain only emerge into the upward hemisphere. In the simplest case it is given by the Lambertian law being independent of the angular argument. For example, an empirical photometric function was proposed by Minnaert (cf. [15]), i.e., the scene bidirectional reflectance factor,

$$\rho(\lambda,e,i) = \rho(\lambda)cos^{k(\lambda)-1}icos^{k(\lambda)-1}e, \quad (4)$$

where λ is the spectral wavelength, k the Minnaert constant being related to the surface roughness, i an incidence angle and e an exitance angle.

Put the emergent radiance I-function of the generalized Chandrasekhar's planetary problem in terms of the three-dimensional scattering function $S(z_1,x,y;\Omega,\Omega_0)$,

$$I(z_1,x,y;\Omega,\Omega_0)=FS(z_1,x,y;\Omega,\Omega_0)/4v. \quad (5)$$

Then, on making use of Eqs.(1)~(3), after somewhat lengthy analytical arguments (cf. [24], [26]), we get the following partial differential-integral equation for the scattering function $S(z_1,x,y,\Omega,\Omega_0)$ as below,

$$\frac{\partial S}{\partial z_1}(z_1,x,y;\Omega,\Omega_0)+(tan\Theta cos\phi+tan\Theta_0 cos\phi_0)\frac{\partial S}{\partial x} +$$
$$+\ (tan\Theta sin\phi+tan\Theta_0 sin\phi_0)\frac{\partial S}{\partial y} +$$
$$+\ \alpha(z_1)\left(\frac{1}{v}+\frac{1}{u}\right)S = \sigma(z_1)\Big[p(z_1;\Omega,-\Omega_0) +$$
$$+\frac{1}{4\pi}\int_{2\pi} S(z_1,x,y;\Omega,\Omega'')p(z_1;-\Omega'',-\Omega_0)\frac{d\Omega''}{v''}$$
$$+\frac{1}{4\pi}\int_{2\pi} p(z_1,\Omega,\Omega')S(z_1,x,y;\Omega',\Omega_0)\frac{d\Omega'}{v'} +$$
$$+\frac{1}{16\pi^2}\int_{-\infty}^{\infty}\int_{-\infty}^{\infty}\int_{2\pi}\int_{2\pi} S(z_1,x-x',y-y';\Omega,\Omega') \times$$
$$\times\ p(z_1;-\Omega',\Omega'')S(z_1,x',y';\Omega'',\Omega_0)dx'dy'$$
$$\frac{d\Omega'}{v'}\frac{d\Omega''}{v''}\Big], \quad (6)$$

together with the initial condition

$$S(z_s,x_s,y_s;\Omega,\Omega_0)=4\rho(z_s,x_s,y_s;\Omega_0,\Omega_s)uv. \quad (7)$$

Even with the aid of high-speed digital computers, it does not seem easy to get the numerical solution of Eq.(6). In the next section it is shown how to get the numerical approximation of the ground albedo in rugged terrain with the aid of the one-dimensional scattering and transmission functions, allowing for the mean adjacent effect. In our preceding papers (cf. [9]), we discussed the boundary condition in terms of the rendering equation governing the Hopf-type of Fredholm integral equation. In next section for reference model rendering is discussed. In the rugged terrain the simultaneous solution of the transfer and rendering equations is not easy in Cartesian coordinates. In section 4 we discuss the approximation, allowing for the adjacent and topographic effect.

MODEL RENDERING

The apparent radiance of high spatial resolution based on surface features by spacecraft depends on a number of factors such as the solar position, atmospheric composition, reflectance of backgrounds surrounding the target (adjacency effects), and the terrain slope. The accurate classification of the sensed radiance data requires the allowance of these effects. Up to now, based on the reasonable atmospheric models, the adjacency effects have been evaluated by allowing not only for the diffuse reflector but also for the non-Lambertian surface. Recently, an allowance of the topographic effect has been approximately taken into account by combining the adjacent effect with the terrain elevation data (cf. [3], [9], [10], [12], [14], [18], [19], [21], [28],).

In general, the atmospheric effect in rugged terrain should be evaluated in allowance with the topographic effect and the bidirectional reflectance law of each target pixel. In other words, the generation of images through application of photon scattering to models of objects and surrounding media is what we refer to here as "model rendering" (cf. [9], [11],). Let us discuss the energy in a radiation field due to emission of light, transmission through a nonhomogeneous nonscattering medium, and multiple reflections at various surfaces in the medium. The aim is to compute the intensity of the radiation coming from various directions and registering in an image plane in certain cells called pixels. It is assumed that phase, frequency and other temporal aspects can be neglected. Let us introduce the functions as below.

$i(\Theta,\varphi)$=intensity of radiation at a point x travelling in a direction whose polar and azimuthal angles are Θ and φ.
Υ=distance between points x' and x,
$\rho(x,x',x'')$=fraction of light travelling from a surface element at x'' and arriving at a surface element at x that is scattered by a surface element at x',

$e(x,x')$=energy per unit time per unit area at x due to energy emitted at x',

$g(x,x')$=geometric factor that takes into account intervisibility between points x' and x' as well as the spreading of energy from a point source:
= 0, if there is no clear line of sight between x and x',
$=1/\tau^2$, otherwise, where τ is the distance between x and x'.

Introducing the function I which is a measure of the radiation at x due to radiation coming from x',

$$I(x,x')=i(\Theta',\varphi')\cos\Theta\cos\Theta'/\tau^2, \tag{8}$$

then, I governs the integral equation

$$I(x,x')=g(x,x')+\left\{e(x,x')+\int_s \rho(x,x',x'')I(x',x'')dx''\right\}. \tag{9}$$

The integral is over S, all the surfaces of all the objects in the problem.

This discussion is based on Kajiya ([11]), who calls I the transport intensity. The quantity I has units of energy per unit time per unit area of source per unit area of the scatterer. If the medium between surfaces participates in the scattering, then the intensity of radiation satisfies an integro-differential equation (see, [1], [5], [12]).

Approximate solutions: There are various approximations to the solution of the integral equation. The integral equation is approximated as a sum and the resultant linear algebraic equations are solved via infinite series, orders of scattering, and "ray tracing". It should be noted that these approximations do not attempt to compute the total radiation field but, rather, they only determine the components due to one scattering, two scatterings, etc.

In the case of diffuse reflector, the radiosity approximation is useful, because the surfaces have not angular dependence on the bidirectional reflectance function. Then the radiosity $B(x')$, is defined to be

$dB(x')$ = dx' integral over hemisphere $[I(\Theta',\phi')\cos\Theta']dw$

= dx' integral over $S[I(x,x')]dx$.

The radiosity is determined by computing the total integrated intensity. This is an intensive computation because of involving numerous intervisibility calculations. The integral equation was solved by a Monte Carlo method with multidimensional sequential sampling by Kajiya whose results were compared with the ray tracing approximation.

In our preceding paper (cf. [9]), we discussed the boundary condition in terms of the rendering equation governing the Hopf-type integral equation. Even though in the rugged terrain the Neumann solution of the rendering equation can be approximated by a few terms, the simultaneous solution of the transfer and rendering equations is not so easy in Cartesian coordinates. Then, in next section we discuss an approximation for the adjacent and topographic effects.

ATMOSPHERIC CORRECTION IN RUGGED TERRAIN

In general, the atmospheric effect in rugged terrain should be estimated in allowance with the bidirectional reflectance law of each target pixel in association with the revised rendering equation. In other words, the bidirectional spectral reflectance law depends on the terrain elevation and position, polar and azimuthal angles of the normal to the surface in a pixel, the angles of incidence and reflection in a pixel.

To evaluate exactly the atmospheric effect in rugged terrain is very difficult. In this section, we approximate the atmospheric and topographic effects by ignoring variations in ground reflection due to the inclination of the target. Based on Lowtran standard atmospheric model ([4]), the scattering and transmission functions have been evaluated.

Defining the mean adjacent effect, we have the following approximation for the target ground albedo A_t ([9]):

$$A_t = [I_{obs}-(P-V)\bar{A}^2-(Q-W)\bar{A}-R)]/X \tag{10}$$

$$X = e^{\tau}[B(\Upsilon,v)\Upsilon\pi Fe^{-\tau/u}+\frac{F}{4v}\int_0^{2\pi}\int_0^1 T(\tau;w,u,\phi'-\phi_0) \times B(\Upsilon(w,v))\Upsilon(w,v)dwd\phi'], \tag{11}$$

Where $\bar{A}$ is the mean background albedo, $B(\Upsilon,v)$ is the bidirectional reflectance distribution function due to Minnaert, $J_s,L_t,P,Q,R,V,$ and W are respectively radiance coefficients which can be computed from the S-, S^*-, and T-functions as below (cf. Kawata et al. 1988 [13]).

Thus

$$\bar{A} = -Q+\sqrt{Q^2-4P(R-I_{obs})}/2P, \tag{12}$$

$$B(\Upsilon,v)=(k+1)(\Upsilon v)^{k-1}/2\pi, \tag{13}$$

$$\Upsilon = \begin{cases} \cos\Theta & \text{for} \quad \cos\bar{\Theta} \geq 0, \\ 0 & \text{for} \quad \cos\bar{\Theta} \leq 0, \end{cases} \tag{14}$$

$$\cos\bar{\Theta} = uv+\sqrt{1-u^2}\sqrt{1-v^2}\cos(\phi_n-\phi_0), \tag{15}$$

$$R=FS(\tau;\Omega,\Omega_0)/4v, \tag{16}$$

$$W=\exp\left\{\frac{-\tau}{v}\right\} L_t, \tag{17}$$

$$L_t=\left\{u\exp\left\{\frac{-\tau}{u}\right\}+\frac{1}{4\pi}\int_{2\pi} T(\tau;\Omega',\Omega_0)d\Omega'\right\}, \tag{18}$$

$$Q=\left\{\exp\left\{\frac{-\tau}{v}\right\}+\frac{1}{4\pi v}\int_{2\pi} T^*(\tau;\Omega',\Omega_0)d\Omega'\right\} L_t, \tag{19}$$

$$P=\frac{1}{4\pi^2}\left\{\exp\left\{\frac{-\tau}{v}\right\}+\frac{1}{4\pi v}\int_{2\pi} T^*(\tau;\Omega',\Omega_0)d\Omega'\right\} J_sL_t \quad , \tag{20}$$

$$J_s=\int_{2\pi}\int_{2\pi} S^*(\tau;\Omega',\Omega'')d\Omega'd\Omega'', \tag{21}$$

$$V=\frac{\exp(-\tau/v)}{4\pi^2} J_sL_t. \tag{22}$$

Furthermore I_{obs} is the observed radiance at top, S- and T-functions are respectively the scattering and transmission functions.

Thus the $\cos^{-1}v$ is the zenith angle of the normal to the target surface, ϕ is the azimuthal angle of incoming radiation, and ϕ_n is the direction of the maximum slope at the target.

If we denote the tilt angle of the target surface as α, then we have $\Theta_n=\alpha$. Since the values of α and ϕ_n can be computed from the elevation data for a given rugged terrain, we can obtain the values of Υ at each target location, those values depend on the height of the target, whereas in Eq. (14) the explicit dependence on the height of the target does not appear. In a flat terrain we have $\Upsilon=u$ because $\alpha=0$. The zero value of Υ corresponds to the case where no direct solar illumination is available at the target point.

The S- and T-functions in Eqs. (10) and (11) are the initial value solutions of the following Riccati type of nonlinear integro-differential equations, whose numerical values can be obtained with the aid of the high-speed electronic computers (cf. [1], [7], [21]).

$$\left\{\frac{1}{v}+\frac{1}{u}\right\} S(\tau;\Omega,\Omega_0) + \frac{S}{\tau} = \lambda(\tau)\left[p(\tau;\Omega,-\Omega_0) + \frac{1}{4\pi}\int_{2\pi} p(\tau;\Omega,\Omega'')S(\tau;\Omega'',\Omega_0)\frac{d\Omega''}{v''} + \frac{1}{4\pi}\int_{2\pi} S(\tau;\Omega,\Omega')p(\tau;-\Omega',-\Omega_0)\frac{d\Omega'}{v'} + \frac{1}{16\pi^2}\int_{2\pi}\int_{2\pi} S(\tau;\Omega,\Omega')p(\tau;-\Omega',\Omega'') \times S(\tau;\Omega'',\Omega_0)\frac{d\Omega' d\Omega''}{v'v''}\right], \quad (23)$$

$$\frac{\partial}{\partial\tau}S^*(\tau;\Omega,\Omega_0) = \lambda(\tau)\left\{p(\tau;\Omega,-\Omega_0)\exp\left[-\tau\left\{\frac{1}{v}+\frac{1}{u}\right\}\right] + \frac{\exp(-\tau/u)}{4\pi}\int_{2\pi} T(\tau;\Omega,\Omega')p(\tau;-\Omega',\Omega_0)\frac{d\Omega'}{v'} + \frac{\exp(-\tau/v)}{4\pi}\int_{2\pi} p(\tau;\Omega,-\Omega'')T^*(\tau;\Omega'',-\Omega_0)\frac{d\Omega''}{v'} + \frac{1}{16\pi^2}\int_{2\pi}\int_{2\pi} T(\tau;\Omega,\Omega)p(\tau;-\Omega',-\Omega'') \times T^*(\tau;\Omega'',\Omega_0)\frac{d\Omega' d\Omega''}{v'v''}\right\} \quad (24)$$

$$\frac{1}{v}T(\tau;\Omega,\Omega_0) + \frac{\partial T}{\partial\tau} = \lambda(\tau)\left[\exp\left\{\frac{-\tau}{u}\right\}p(\tau;-\Omega,-\Omega_0) + \frac{1}{4\pi}\int_{2\pi} p(\tau;-\Omega,-\Omega'')T(\tau;\Omega'',\Omega_0)\frac{d\Omega''}{v''} + \frac{\exp(-\tau/u)}{4\pi}\int_{2\pi} S(\tau;\Omega,\Omega')p(\tau;\Omega',-\Omega_0)\frac{d\Omega'}{v'} + \frac{1}{16\pi^2}\int_{2\pi}\int_{2\pi} S(\tau;\Omega,\Omega')p(\tau;\Omega',-\Omega'') \times T(\tau;\Omega'',\Omega_0)\frac{d\Omega' d\Omega''}{v'v''}\right], \quad (25)$$

In Eqs. (23) through (25) τ is the optical thickness

$$\tau = \int_0^{z1} \alpha(z)dz, \quad (26)$$

and $\lambda(t)$ is the ratio of the scattering and transmission coefficients, i.e., $\lambda=\sigma/\alpha$.

Equations (25), (26) and (27) should be solved subject to the initial conditions

$$S(0;\Omega,\Omega_0) = 0, \qquad T(0;\Omega,\Omega_0) = 0 \quad (27)$$

and

$$S^*(0;\Omega,\Omega_0) = 0, \qquad T^*(0;\Omega,\Omega_0) = 0 \quad (28)$$

Furthermore, the S, T, S^* and T^* functions satisfy the reciprocity relations

$$S(\tau;\Omega,\Omega_0)=S(\tau;\Omega_0,\Omega), \quad S^*(\tau;\Omega,\Omega_0)=S^*(\tau;\Omega_0,\Omega) \quad (29)$$

and

$$T(\tau;\Omega,\Omega_0)=T^*(\tau;\Omega_0,\Omega). \quad (30)$$

It should be noted that the bidirectional reflection law and the rendering equation have not been analytically taken in to account for the above discussion. In our later paper an interaction of the scattered and reflected radiation on the rugged terrain will be analytically discussed.

Eq. (10) is the basic equation which removes both the atmospheric and topographic effects from the Landsat data covering a rugged terrain, whereas the adjacent effect due to the background albedos has not been allowed for. Eqs. (10) and (11) have been used for the production of a shaded relief image in the classification ground albedo map from the Landsat Computer Compatible Tape in the Kanazawa area, Japan. It provides a good example for qualitative analysis.

APPLICATION AND RESULTS

In order to test the Minnaert assumption by our radiometric correction model, we selected the mountainous area near Kanazawa City, Ishikawa Prefecture, Japan. The elevations of the study site range from about 300m to 1600m. The Marine Observation Satellite (MOS-1) MESSR data taken on June 18, 1987 was used in this analysis. The MOS-1 MESSR has the same wavelength bands as Landsat MSS with the spatial resolution of 50m. The solar zenith angle at data acquisition was 24 degrees; solar azimuth was 117 degrees. Within the study site there are three small lakes. A 320 x 390 Digital Terrain Model (DTM) with the same grid size of MESSR data was used for the geometric rectification. This DTM was made at our laboratory by digitizing the geographic map of the study site published by National Geographic Institute of Japan (a scale of 1:25000). A midlatitude summer model and a rural aerosol model with a horizontal visibility of 23km (corresponding to a clear sky) are adopted in the computation of R and T functions, and radiance coefficients. The atmospheric parameters for these models were obtained from Lowtran 6 code (Kneizys et al. 1983).

Figure 2 is the histogram equalized image of the study site (320x290 pixels) with 16 gray levels based on original band 4 data (showing strong topographic effects) of MOS-1. In the case of Minnaert model we need to determine an appropriate value of Minnaert coefficient k. Because the variations in observed radiances in mountainous areas are believed to be primarily due to changes in slope inclination at the reflecting target, we can expect to have a constant albedo for forests of a single species after the removal of the topographic effect is done. We compute average albedos and its standard deviations of a selected brown birch forest area (located in the center of the study site) for different values of k between 0 and 1. The appropriate value of k is so chosen that we have a minimum standard deviation in albedo estimation of such selected area. We found k=0.63 for band 4 as an appropriate Minnaert coefficient for a brown birch forest. The computed albedo distribution image based on the Minnaert reflection model with k=0.63 is shown in Figure 3. In this albedo image the removal of the topographic effects is successfully demonstrated. The computed albedo cross section (dotted line) along the 167th line, together with the CCT data cross section (solid line) along the same line are shown in Fig. 4. From this figure we can see a considerable flat albedo cross section along this line with a mean albedo A=0.53. This result is quite reasonable, because the ground cover along this line is a single category of brown birch forest. The foregoing results indicate the reflection by rugged terrain vegetation (mostly deciduous forest) follows Minnaert's law, rather than Lambert's law.

The conclusions of this study are as follows:

1) In this study we have developed a new analytical correction method for rugged terrain data which allows the use of the more general Minnaert reflection law at the ground surface.
2) We demonstrated the validity of the proposed method for the MOS-1 MESSR image data.
3) We found that the reflection by rugged terrain vegetation (mostly deciduous forest) follows Minnaert's law, rather than Lambert's law.

DISCUSSION

In this paper, based on the multidimensional theory of radiative transfer in the vertically heterogeneous atmosphere bounded by the vertically and horizontally inhomogeneous background, we discussed analytically and approximately the reflection of radiation by rugged terrain vegetation (mostly deciduous forest) based on Minnaert's law. The validity of the proposed method for the MOS-1 MESSR image data is shown. In other words, it is shown that the multidimensional theory of radiative transfer is useful for the analysis of multispectral data obtained from space.

REFERENCES

[1] Busbridge, I.W. 1960. The Mathematics of Radiative Transfer, Cambridge University Press, London.

[2] Crosbie, A.L., and Schrenker, R.G. 1982. Exact expressions for radiative transfer in a Three-dimensional rectangular geometry. JQSRT, 28, pp. 507-526.

[3] Dinner, D.J., Martonchik, J.V., Danielson, E.D., and Brugge, C.J. 1989. Atmospheric correction of high resolution land surface images. IEEE IGARSS'89, pp. 860-863.

[4] Kneizys, F.X., Shettle, E.P., Gallery, W.O., Chetwynd, J.H. Jr., Abreu, L.W., Selby, J.E.A., Clough, S.A., and Fenn, R.W., 1983. Atmospheric Transmittance Radiance: Computer code Lowtran. AFGL-TR-83-0187, AIR FORCE GEOPHYSICS LABORATORY, Hanscom AFB, MASS.

[5] Fraser, R.S., Ferrare, R.A., Kaufman, Y.J., and Markham, B.L. 1992. Algorithm for atmospheric corrections of aircraft and satellite imagery. Int.J.Remote Sensing, Vol. 13, pp. 541-557.

[6] Haan, J.F.de., Hovenier, J.W., Kokke, J.M.M. and Stokkom, H.T.C. van. Removal of atmospheric influences on satellite-borne imagery: a radiative transfer approach. 1991. Remote Sens. Environ. Vol. 37, pp. 1-21.

[7] Kagiwada, H.H., Kalaba, and Ueno, S. 1975. Multiple Scattering Processes: Inverse and Direct. Addison-Wesley Publ. Co., Reading Mass.

[8] Kagiwada, H., Kalaba, R., Timko, S., and Ueno, S. 1990. Associate memories for system identification: inverse problems in remote sensing. Math. Comput. Modelling. Vol. 14, pp.-200-202.

[9] Kagiwada, H., Ueno, S., and Kawata, Y. 1990. Analytical approach to the simulation of the atmospheric and topographic effects in remote sensing from space. IEEE IGARSS'90, pp. 183-186.

[10] Kagiwada, H.H., Ueno, S., and Kawata, Y. 1991. Approximation of topographic effect on atmospheric correction in rugged terrain. IEEE IGARSS'91, pp. 665-668.

[11] Kaufman, Y.J., and Fraser, R.S. 1984. Atmospheric effect on classification of finite field, Remote Sens. Environm., 15, pp. 95-118.

[12] Kawata, Y., Ueno, S., and Kusaka, T. 1988. Radiometric correction for atmospheric and topographic effects on Landsat MSS image. Int. J. Remote Sensing, Vol. 9, pp. 729-748.

[13] Kawata, Y., Ohtani, A., Kusaka, T., and Ueno, S. 1989. On the classification accuracy for the MOS-1 MESSR data before and after the atmospheric correction. IGARSS'89, Vol. 2., pp. 802-805.

[14] Kawata, Y., Hatakeyama, A.H., Kusaka, T., and Ueno, S. 1992. The evaluation of various radiance components in mountainous terrain. To appear in Proc. of IEEE IGARSS;92, Houston, USA.

[15] Minnaert, M. 1961. Photometry of the moon, in Solar System, Vol. III, Planets and Satellites, G.P. Kuiper and B.M. Middlehurst, Eds. Chicago, Univ. Chicago Press, pp. 213-248.

[16] Odell, S.R., and Weinman, J.A., 1975. The effect of atmospheric haze on image of the earth's surface, J. Geophys. Res., 80, pp. 5035-5040.

[17] Otterman, J., and Fraser, R.S., 1979, Adjacency effects on imaging by surface reflection and atmospheric scattering. Appl. Opt., 18, pp. 2852-2869.

[18] Proy, C., Tanre, D., and Deschamps,, P.Y. 1989. Evaluation of topographic effects in remotely sensed data. Remote Sens. Environ. 30, pp 21-32.

[19] Ranson, K.J., Irons, J.R., and Danghtry, C.S.T. 1991. Surface albedo from bidirectional reflectance. Remote Sens. Environ. Vol. 35, pp. 201-211.

[20] Sobolev, V.V., 1975, Light Scattering in Planetary Atmospheres (Translated by W. Irvine). Pergamon Press, Oxford.

[21] Tanre, D., Herman, M., and Deshamps, P.Y., 1981, Influence of background contribution upon space measurements of ground reflectance, Appl. Apt. 20, pp. 3676-3684.

[22] Woodham, R.J., and Gray, M.H., 1987. An analytic method for radiometric correction of satellite multispectral scanner data. IEEE Trans, Geosci. Remote Sensing. Vol. GE-25, pp. 258-271.

[23] Ueno, S., 1960, The probabilistic method for problems of radiative transfer: X. Diffuse reflection and transmission in a finite inhomogeneous atmosphere. Astrophys. J., 124, pp. 729-745.

[24] Ueno, S., 1982, Remote sensing-research experience and problems, in Marine Remote Sensing (Eds. Vernberg, F.J., and Diemer, F.D.), Univ. S. Carolina Press, pp. 451-510.

[25] Ueno, S., Haba, Y., Kawata, Y., Kusaka, T., and Terashita, Y., 1979, The atmospheric blurring effect on remotely sensed earth imagery, in Remote Sensing of Atmosphere (Eds. Fymat, A.L., and Zuev, V.E.). Elsevier Sci. Publ. Co., pp. 305-310.

[26] Ueno S., and Kawata, Y., 1987, Earth-Atmosphere System: Identification of Optical Parameters, in Encyclopedia of Systems and Control (Ed. Singh, M.), Pergamon Press, pp. 1307-1311.

[27] Ueno, S., Kawata, y., and Kusaka, T., 1987,

Ground Albedo Mapping: Invariant Embedding. Ibid., Pergamon Press, pp. 2046-2053.

[28] Ueno S., Kawata, Y., Kusaka, T., and Takashima, T. 1988. on the Retrieval of the Atmospheric and Topographic Effects on Landsat MSS Imagery. In "Current Problems in Atmospheric Radiation", (Edited by J. Lenoble and J.F. Gelyn). A. Deepack Publishing, 1989, pp. 481-483.

[29] Ueno, S., Kawata, Y., and Kusaka, T., 1988, Comparative analysis of Landsat-5 and SPOT HRV data in Kanazawa region, in Proc. of 16th Congress of International Society for Photogrammetry and Remote Sensing (ISPRS), July 1-10, 1988, Kyoto, Japan, VII, pp. 651-662.

[30] Ueno, S., Kawata, Y., and Kusaka, T., 1989, Landcover analysis of multitemporal Thematic Mapper data. In Proc. of IGARSS'89, July 10-14, 1989, Vancouver, Canada, pp. 802-805.

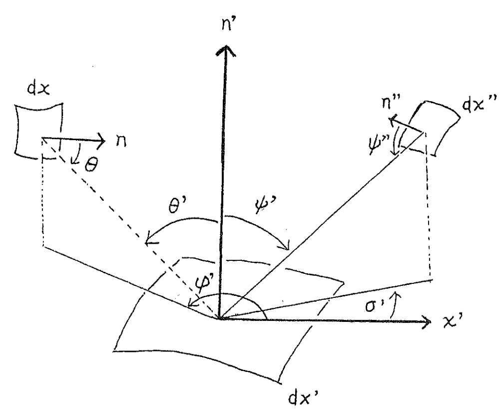

Fig. 1 Diffuse reflection of rays at targets.

Fig. 3 The same as Fig. 2, except it is based on the computed albedo values by assuming Minnaert reflection law with k=0.63

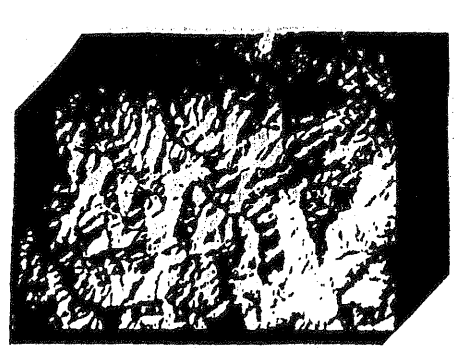

Fig. 2 The band 4 image of the study site with 16 gray levels taken on June 18, 1987 by MOS-1

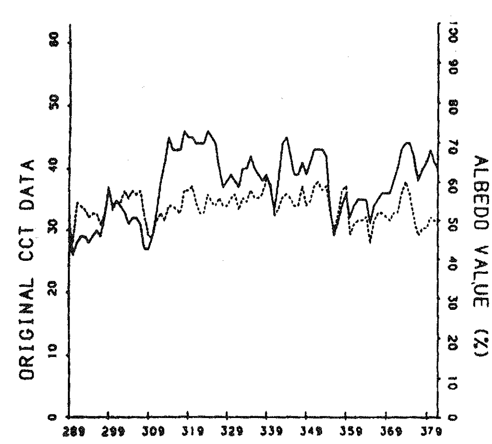

Fig. 4 The ground albedo cross section (dotted line) along the 167th line, together with the CCT data cross section (solid line) along the same line. The horizontal axis represents the column number. The vertical axis represents either the digital count for the solid line or the albedo value in percentages for the dotted line.